

1 **Reporter gene assay for membrane fusion of extracellular vesicles**

2

3 Masaharu Somiya <sup>1,\*</sup>, and Shun'ichi Kuroda <sup>1</sup>

4 <sup>1</sup>*The Institute of Scientific and Industrial Research, Osaka University, Osaka 567-0047,*

5 *Japan*

6

7 \*Corresponding author: Prof. Masaharu Somiya, Ph.D

8 Department of Biomolecular Science and Reaction, The Institute of Scientific and

9 Industrial Research, Osaka University, 8-1 Mihogaoka, Ibaraki, Osaka 567-0047, Japan

10 E-mail: [msomiya@sanken.osaka-u.ac.jp](mailto:msomiya@sanken.osaka-u.ac.jp)

11 Phone: 81-6-6879-8462

12

13

14 **Abstract**

15 Extracellular vesicles (EVs) secreted by living cells are expected to deliver biological  
16 cargo molecules, including RNA and proteins, to the cytoplasm of recipient cells. There  
17 is an increasing need to understand the mechanism of intercellular cargo delivery by EVs.  
18 However, the lack of a feasible bioassay has hampered our understanding of the biological  
19 processes of EV uptake, membrane fusion, and cargo delivery to recipient cells. Here, we  
20 describe a reporter gene assay that can measure the membrane fusion efficiency of EVs  
21 during cargo delivery to recipient cells. When EVs containing tetracycline transactivator  
22 (tTA)-fused tetraspanins are internalized by recipient cells and fuse with cell membranes,  
23 the tTA domain is exposed to the cytoplasm and cleaved by protease to induce  
24 tetracycline responsive element (TRE)-mediated reporter gene expression in recipient  
25 cells. This assay (designated as **EV-mediated tetraspanin-tTA delivery assay, ETTD**  
26 **assay**), enabled us to assess the cytoplasmic cargo delivery efficiency of EVs in recipient  
27 cells. With the help of a vesicular stomatitis virus-derived membrane fusion protein, the  
28 ETTD assay could detect significant enhancement of cargo delivery efficiency of EVs.  
29 Furthermore, the ETTD assay could evaluate the effect of potential cargo delivery  
30 enhancers/inhibitors. Thus, the ETTD assay may contribute to a better understanding of  
31 the underlying mechanism of the cytoplasmic cargo delivery by EVs.

32

33 **Keywords:** cargo transfer; extracellular vesicles; membrane fusion; NanoLuc; VSV-G

34

## 35 **Introduction**

36 Extracellular vesicles (EVs) are secreted by living cells and contain biomolecules derived  
37 from the donor cells. The physiological role of EVs remains largely unknown and they  
38 were formerly known as the “garbage bin” of cells for excretion of the unwanted  
39 molecules or organelles. Several studies have shown the cellular disposal role of EVs <sup>1,2</sup>  
40 although a vast majority of current EV research focuses on the cargo delivery of EVs.  
41 Since EVs contain cargo proteins and RNAs, their contents can be transferred from a  
42 donor cell to a recipient cell via a paracrine or endocrine mechanism. Recently, EV-  
43 mediated cargo delivery events in pathophysiological settings, such as cancers, have  
44 attracted considerable attention. Several studies have reported that EVs are involved in  
45 tumor suppression <sup>3,4</sup> and tumor progression <sup>5,6</sup>. Several studies have demonstrated that  
46 EVs can deliver small RNAs to recipient cells and elicit phenotypic changes. However,  
47 there is limited evidence that demonstrates cargo delivery by EVs into recipient cells <sup>7</sup>.  
48 Many confounding factors in the experimental conditions and contaminants in the EV  
49 fraction <sup>8</sup> must be taken into account in the cargo delivery experiments, to draw a  
50 conclusion on “EV cargo transfer hypothesis” <sup>9</sup>.

51 The main challenge in current EV research is the lack of a feasible and reliable  
52 assay to evaluate the functional cargo delivery process in the recipient cells <sup>9,10</sup>. Several

53 reporter assays that demonstrate the functional delivery of cargo proteins or RNAs have  
54 been reported, including miRNA<sup>11,12</sup>, Cre-LoxP<sup>13,14</sup>, and CRISPR/Cas9-gRNA reporters  
55<sup>15</sup>. However, these assays are influenced by various confounding factors including non-  
56 EV components in the EV fraction. Although the readout of these assays is informative  
57 for deciphering the delivery mechanism of EVs in recipient cells, a more precise reporter  
58 assay is needed. Mechanistically, cytoplasmic cargo delivery should occur after  
59 endocytosis and subsequent membrane fusion, or direct fusion with the plasma membrane  
60<sup>16</sup>. Upon membrane fusion, the luminal side of EVs is exposed to the cytoplasm of  
61 recipient cells and release their cargo. The functional delivery assay should reflect the  
62 biological delivery mechanism, especially membrane fusion of EVs.

63 In this study, we developed a reporter assay to quantify the membrane fusion of  
64 EVs in recipient cells. In this assay, following fusion of EVs with the cell membrane of  
65 the recipient cells, a transcription factor is released from the EVs and then upregulates  
66 the expression of a reporter gene (luciferase or fluorescence protein). This assay provides  
67 a biologically orthogonal readout and enables us to accurately interpret the cargo delivery  
68 process of EVs.

69

70

## 71 **Materials and Methods**

### 72 *Materials*

73 The chemical reagents and antibodies used in this study are listed in Supplementary Table

74 1. All NanoLuc substrates were purchased from Promega. The plasmids used in this study

75 are listed in Supplementary Table 2 and deposited at Addgene. Plasmids were constructed

76 using PCR-based methods (Gibson Assembly<sup>17</sup>) and confirmed by Sanger sequencing.

77

### 78 *Cell culture and transfection*

79 Human embryonic kidney HEK293T cells (RIKEN Cell Bank) were maintained in 10%

80 (v/v) fetal bovine serum (FBS)-containing Dulbecco's modified Eagle's medium

81 (DMEM) supplemented with 10 µg/mL penicillin-streptomycin solution. Cells were

82 cultured at 37°C under 5% CO<sub>2</sub> in humidified conditions.

83 Transfection of HEK293T cells was performed as follows: cells were plated in a

84 cell culture dish or multi-well plate and cultured overnight. The next day, the cells were

85 transfected using 25-kDa branched polyethyleneimine (PEI, Sigma). The ratio of plasmid

86 DNA to PEI was 1: 4 (weight). After 24–96 h, the cells were used in the subsequent

87 experiments. Cell culture supernatant was collected after 2–4 days and centrifuged at

88 1,500 ×g for 5 min to remove cell debris.

89

90 *NanoLuc assay*

91 To quantify the expression level of the reporter NanoLuc, the transfected cells were lysed  
92 and mixed with NanoLuc substrate (Nano-Glo Luciferase Assay System; Promega)  
93 according to the manufacturer's instructions. Luminescence signal from the cell lysate  
94 was measured by using a plate reader, Synergy 2 (BioTek).

95

96 *Characterization of tTA-fused proteins in cell lysate and EVs*

97 Protein expression was assessed by western blotting. Briefly, lysates of the transfected  
98 cells (total protein was extracted using radioimmunoprecipitation assay [RIPA] buffer  
99 [Nacalai Tesque] containing a protease inhibitor cocktail [Nacalai Tesque]) or the  
100 supernatant was mixed with reductant-free sample buffer and incubated at room  
101 temperature for 20 min. Proteins were separated by sodium dodecyl sulfate  
102 polyacrylamide gel electrophoresis (SDS-PAGE) and transferred to polyvinylidene  
103 difluoride (PVDF) membrane. Proteins on the membrane were detected using antibodies  
104 (Supplementary Table 1) and ImmunoStar LD reagent (FUJIFILM Wako Pure Chemical).  
105 As a loading control for cell lysates, the membrane was probed with anti-GAPDH  
106 antibody.

107

108 *Concentration of EVs*

109 EVs were concentrated by PEG precipitation. The supernatant was mixed with 4× PEG

110 solution (40% PEG 6000 [w/v], 1.2 M NaCl, 1 × PBS [pH 7.4]), and kept at 4°C overnight.

111 The next day, the supernatant was centrifuged at 1,600 ×g for 60 min to pellet the EVs.

112 After decantation, the pellet was resuspended in PBS. Typically, 5–10 mL of the

113 supernatant was concentrated to 100–200 μL.

114

115 *Reporter assay*

116 For the membrane fusion reporter assay, recipient HEK293T cells (10<sup>4</sup> cells/well in 96-

117 well plate) were transfected with plasmids encoding tobacco etch virus (TEV) protease

118 (TEVp) and TRE3G-NlucP (PEST motif-fused NanoLuc [NlucP]<sup>18</sup> under tetracycline

119 responsive element [TRE] promoter), and cultured overnight. The next day, the recipient

120 cells were treated with donor culture supernatant or concentrated EVs and further

121 incubated at 37°C for up to 26 h. To assess the effect of various compounds on membrane

122 fusion efficiency, recipient cells were treated with the compound 1 h before the addition

123 of supernatant or EVs. After incubation (2–26 h), the expression of NanoLuc in the

124 recipient cells was measured as described above.



125 Reporter expression in recipient cells was also evaluated using an enhanced  
126 green fluorescent protein (EGFP) gene. Recipient cells ( $10^4$  cells/well in 96-well plate)  
127 transfected with pTetOn-EGFP (EGFP under TRE promoter) and pcDNA3.1-TEVp were  
128 treated with EVs, and then observed under a fluorescence microscope IX70 (Olympus)  
129 after 24 h. Cre recombinase-based reporter assay was performed in the same way;  
130 recipient HEK293T cells were transfected with reporter plasmid (encoding LoxP-flanked  
131 mKate and EGFP under the CMV promoter) and plasmid encoding TEVp, treated with  
132 EVs for 24 h the following day, and then observed under a fluorescence microscope.

133

#### 134 *Statistical analysis*

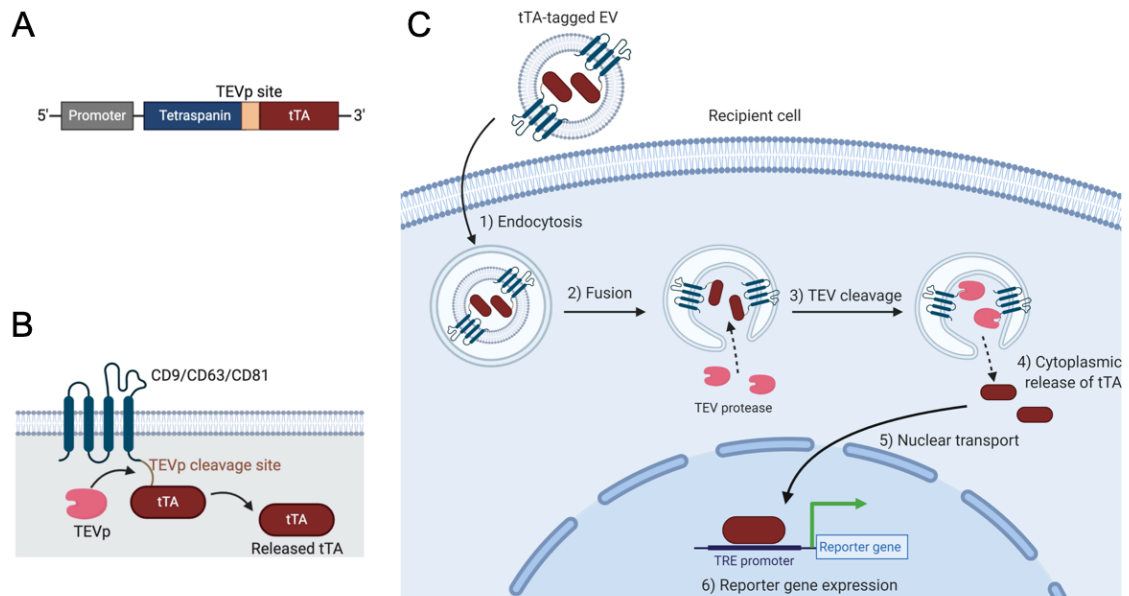
135 Data were analyzed using Student's *t*-test or one-way ANOVA following either *post hoc*  
136 Tukey's HSD or Dunnett's tests. Statistical analysis was performed using the Real  
137 Statistics Resource Pack software created by Charles Zaiontz.

138 **Results**

139 *Characterization of tTA-fused tetraspanins*

140 To establish a reporter assay that can measure the membrane fusion of EVs, we first  
141 prepared plasmids encoding human tetraspanins CD9, CD63, or CD81 with C-terminal  
142 fusion of the TEVp cleavage site, followed by tTA (Fig. 1A). As shown in Fig. 1B, tTA-  
143 fused tetraspanin is cleaved in the presence of TEVp and releases the transcription  
144 activator tTA. When the EVs containing tTA-fused tetraspanin are internalized and fused  
145 with the endosomal membrane, luminal tTA are exposed to the cytoplasmic side, and  
146 TEVp in the recipient cells cleaves the TEVp site, followed by cytoplasmic release of  
147 tTA and induction of the reporter gene expression under the TRE promoter (Fig. 1C). We  
148 designated this assay the **EV-mediated tetraspanin-tTA delivery (ETTD)** assay.

149



150

151 **Fig. 1** Summary of the ETTD assay.

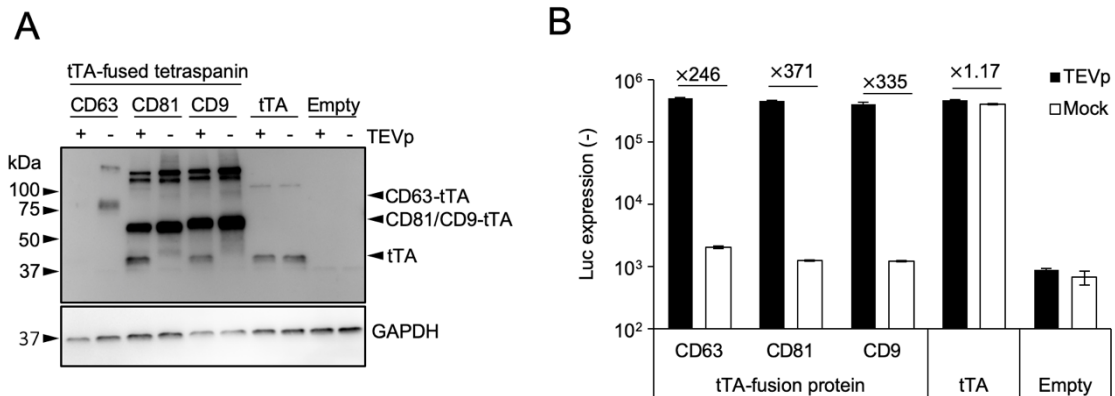
152 (A) Schematic representation of tTA-fused tetraspanin. Tetraspanin and tTA flank a  
153 TEVp recognition site.

154 (B) Topology of tTA-fused tetraspanin protein. Upon the cleavage by TEVp, tTA is  
155 released from membrane-anchored tetraspanin.

156 (C) Schematic representation of the ETTD assay. EV containing tTA-fused tetraspanin is  
157 taken up by cells by endocytosis (1), and fuses with the endosomal membrane (2). After  
158 cleavage by cytoplasmic TEVp (3), tTAs are released into the cytoplasm (4). Released  
159 tTAs are transported to nucleus (5), and induce expression of reporter gene under TRE  
160 promoter (6).

161

162           To demonstrate the feasibility of the above system, HEK293T cells were  
163 transfected with plasmids encoding tTA-fused tetraspanin with or without plasmid  
164 encoding TEVp. As shown in Fig. 2A, the expression of tTA-tetraspanins in the cell lysate  
165 was confirmed by western blotting. In the presence of TEVp, tTA was cleaved and  
166 released from the tTA-fused protein. While CD9 and CD81 showed obvious tTA bands,  
167 CD63 showed only a weak band in the absence of TEVp and no band in the presence of  
168 TEVp. This is probably due to low expression of CD63 in HEK293T cells compared to  
169 CD9 and CD81. When HEK293T cells were transfected with both NlucP (under the TRE  
170 promoter) and tTA-fused proteins, co-expression of TEVp strongly induced Nluc  
171 expression (Fig. 2B), suggesting that tetraspanin-anchored tTA was unable to translocate  
172 into the nucleus, and therefore could not induce reporter gene expression. In contrast,  
173 expression of non-fused tTA protein continually induced reporter gene expression  
174 regardless of the co-expression of TEVp. These results suggest that tTA-fused  
175 tetraspanins induce reporter gene expression in the recipient cells only when the cells  
176 express TEVp.



177 **Fig. 2** Characterization of tTA-fused tetraspanins.

178 (A) Cells were transfected with plasmids encoding tTA-fused tetraspanins and TEVp.

179 After 48 h, cells were lysed and subjected to western blotting. Upper and lower panels

180 represent immunoblotting using anti-TetR antibody and anti-GAPDH antibody,

181 respectively. The expected molecular weights based on the amino acid sequences were as

182 follows: CD63-tTA, 63.2 kDa; CD81-tTA, 63.4 kDa; CD9-tTA, 63.0 kDa; tTA, 36.9 kDa.

183 (B) Expression of NanoLuc under TRE3G promoter in HEK293T cells co-expressing

184 tTA-fused tetraspanins and TEVp. As controls, plasmids encoding tTA without

185 tetraspanin fusion and empty expression plasmid were used. Numbers above the bars

186 indicate the fold increase in NanoLuc expression compared to the mock transfection. N =

187 3, mean ± SD

188

189 To characterize the tTA-fused tetraspanins (CD81 and CD9) in EVs,  
190 supernatants from transfected HEK293T cells were concentrated by PEG precipitation  
191 and analyzed by western blotting (Fig. 3A and 3B). Both tTA-fused CD81 and CD9 were  
192 detected with anti-CD81 and CD9 antibodies, respectively. The tTA-fused proteins were  
193 also detected with an anti-TetR antibody, indicating that the released EVs contain full-  
194 length tTA-fused CD81 or CD9. As a control for the ETTD assay, vesicular stomatitis  
195 virus glycoprotein (VSV-G) was co-expressed in donor cells, as VSV-G is known to  
196 strongly facilitate membrane fusion and subsequent cargo delivery of EVs<sup>19-21</sup>. VSV-G  
197 was detected in the EV fraction, strongly suggesting that released EVs display VSV-G on  
198 their surface along with tTA-fused tetraspanins.

199

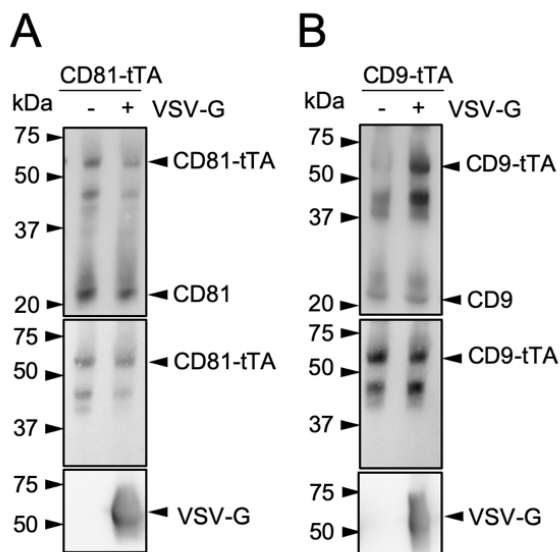


**Fig. 3** Characterization of HEK293T-

derived EVs containing tTA-fused tetraspanins by western blotting.

(A) EVs containing CD81-tTA with or without VSV-G. Antibodies used were as follows; top, anti-CD81 antibody; middle,

206 anti-TetR antibody; bottom, anti-VSV-G antibody.

207 (B) EVs containing CD9-tTA with or without VSV-G. Antibodies used were as follows;

208 top, anti-CD9 antibody; middle, anti-TetR antibody; bottom, anti-VSV-G antibody.

209 The expected molecular weights based on the amino acid sequences were as follows:

210 CD81-tTA, 63.4 kDa; CD9-tTA, 63.0 kDa; VSV-G, 57.7 kDa.

211

212 *Validation of ETTD assay for cargo delivery of EVs*

213 We first attempted to assess whether the unconcentrated cell culture supernatant from

214 donor cells was capable of inducing reporter gene expression in recipient cells. As shown

215 in Fig. 4A, treatment of recipient cells with donor supernatant containing tetraspanin-tTA

216 fusion protein induced reporter gene expression only when the donor cells were

217 transfected with virus-derived fusogenic protein VSV-G. This result suggested that the

218 concentration process is not necessary to evaluate EV membrane fusion in the ETTD

219 assay if the EVs possessed potent fusogenic activity. While the supernatant containing

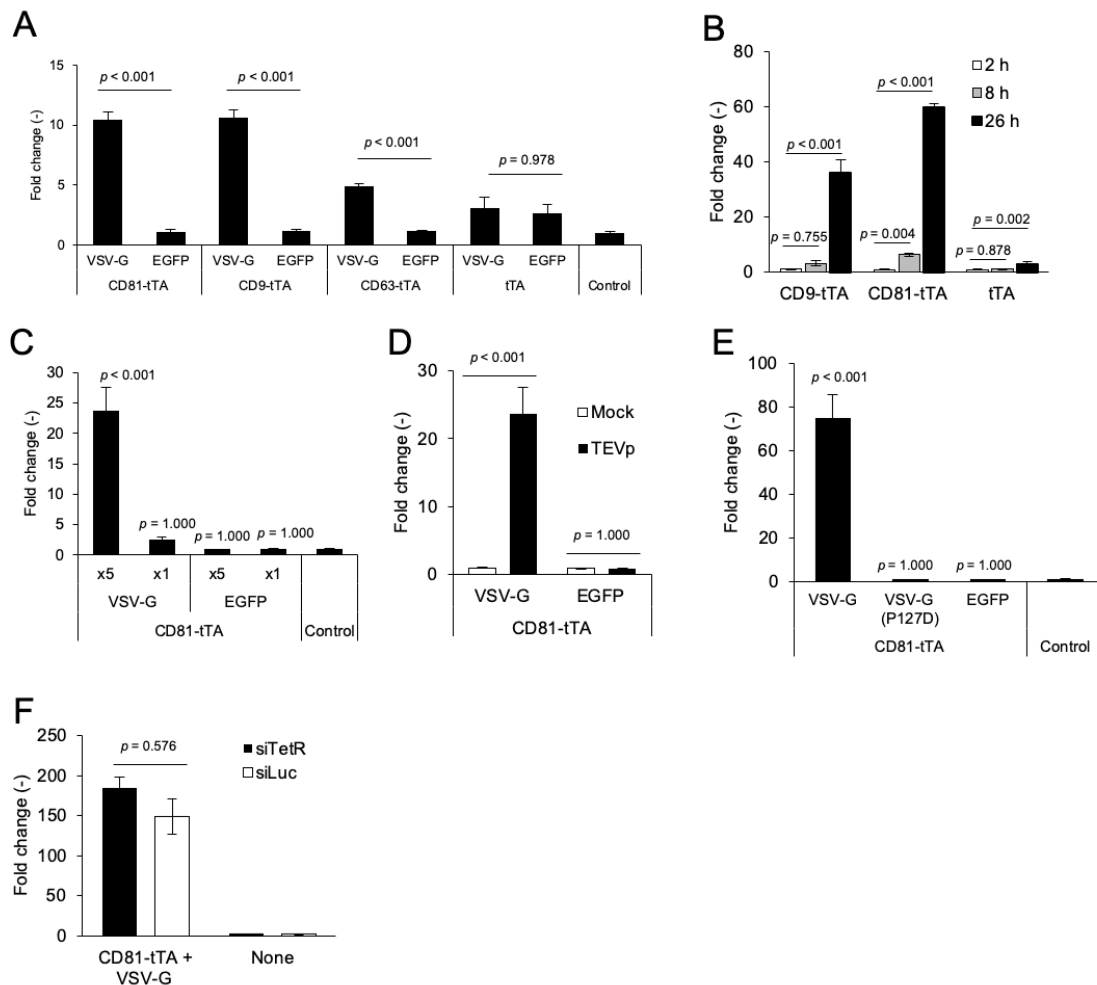
220 tTA-fused CD81 and CD9 induced > 10-fold increase in NanoLuc expression, the

221 supernatant containing tTA-fused CD63 showed less induction (up to 5-fold). This may

222 reflect the lower expression level of tTA-fused CD63 in the donor cells compared to CD9

223 and CD81 (Fig. 2A).

224



225 **Fig. 4** ETTD assay.

226 (A) Donor supernatant was applied to recipient HEK293T cells and NanoLuc expression

227 was measured after 24 h. NanoLuc expression was normalized to the control (treatment

228 with supernatant from non-transfected donor cells).



229 (B) Incubation time-dependent expression of reporter gene. Recipient cells were treated  
230 with concentrated VSV-G-expressing EVs containing tTA-fused CD9 or CD81 for 2, 8,  
231 and 26 h, followed by luciferase assay.

232 (C) Dose-dependent reporter expression in recipient cells. Recipient cells were treated  
233 with EVs containing tTA-fused CD81 with or without VSV-G for 24 h. The relative  
234 amount of EV fraction added was noted as  $\times 1$  or  $\times 5$ .

235 (D) TEVp-dependent reporter gene expression. Recipient cells with or without expression  
236 of TEVp were treated with EVs containing tTA-fused CD81 with or without VSV-G and  
237 subjected to the luciferase assay after 24 h.

238 (E) Effect of fusogenicity deficit VSV-G mutant. Recipient cells were treated with EVs  
239 (tTA-fused CD81) displaying parental VSV-G, mutant VSV-G (P127D), or EGFP for 24  
240 h.

241 (F) Recipient cells were pre-transfected with siRNAs targeting TetR (siTetR) or firefly  
242 luciferase (siLuc), and further treated with EVs containing tTA-fused CD81 and VSV-G  
243 for 24 h.

244 N = 3, mean  $\pm$  SD. Statistical analysis was performed using one-way ANOVA followed  
245 by *post hoc* Tukey's HSD (A, B, D, E, and F) or Dunnett's tests (C).

246

247 Next, we used EVs concentrated by PEG precipitation for the ETTD assay.

248 Recipient cells were treated with EVs for 2, 8, and 26 h and the reporter NanoLuc

249 expression was measured (Fig. 4B). NanoLuc expression gradually increased over time

250 and reached a highest level at 26 h. The expression of NanoLuc was detected as early as

251 8 h. Induction of NanoLuc expression was dependent on the presence of VSV-G and the

252 dose of EVs (Fig. 4C). Fig. 4D indicates that expression of TEVp in the recipient cells

253 was crucial for reporter gene expression, demonstrating that the ETTD assay worked as

254 expected (Fig. 1C). Furthermore, the EVs harboring fusion-deficient mutants of VSV-G

255 (P127D)<sup>19,22</sup> lost the membrane fusion ability of EVs in the assay compared to the EVs

256 harboring parent VSV-G (Fig. 4E), strongly supporting that this assay depicted the

257 membrane fusion-mediated cargo delivery of EVs. Furthermore, absence of VSV-G led

258 to no functional delivery (Fig. 4C to 4E), indicating the poor cargo delivery efficacy of

259 authentic EVs. In addition to HEK293T cells, HeLa cells were used as alternative

260 recipient cells, and similar results were observed, indicating that the ETTD assay is

261 potentially applicable to other cell lines (Fig. S1).

262           It was postulated that the excess of expression plasmid remaining in the  
263 supernatant or mRNA of tTA-fused tetraspanin encapsulated in EVs may induce the  
264 reporter gene expression in the recipient cells, which could confound the bona fide  
265 reporter expression due to the tTA release of EVs. Therefore, we transfected the reporter  
266 cells with siRNA targeting TetR, the TRE-binding domain of tTA to verify that the  
267 reporter gene expression was induced by tTA protein. First, we verified that siRNA  
268 targeting TetR (siTetR) efficiently knocked down tTA (Fig. S2A). Furthermore,  
269 knockdown of tTA by siRNA significantly suppressed TRE-mediated reporter gene  
270 expression (Fig. S2B). Based on these results, siRNA targeting tTA should abrogate the  
271 confounding factors in the ETTD assay, namely, the excess of expression plasmid  
272 remaining in the donor supernatant and mRNA-mediated expression of tTA. After  
273 transfection of siRNA into recipient cells, we applied tTA-fused EVs to recipient cells.  
274 As shown in Fig. 4F, transfection of siRNA targeting tTA showed no effect on the reporter  
275 gene expression, strongly suggesting that the assay readout of the ETTD assay was solely  
276 driven by tTA proteins, neither mRNA nor leftover plasmid DNA.

277

278 *Effect of small molecules on the membrane fusion efficiency of EVs*

279 As the novel ETTD assay can evaluate the membrane fusion efficiency of EVs, we next  
280 examined the effect of potential delivery enhancers and entry inhibitors. According to a  
281 previous report, chloroquine enhanced Cre protein delivery of EVs by disrupting  
282 endosomes and lysosomes using the Cre-LoxP reporter assay <sup>14</sup>. In our reporter assay,  
283 chloroquine treatment did not induce any reporter gene expression (Fig. 5A), suggesting  
284 that chloroquine does not enhance cytoplasmic cargo delivery of EVs. This is probably  
285 because chloroquine treatment induces the destabilization of endosomes/lysosomes and  
286 does not enhance membrane fusion.

287

288

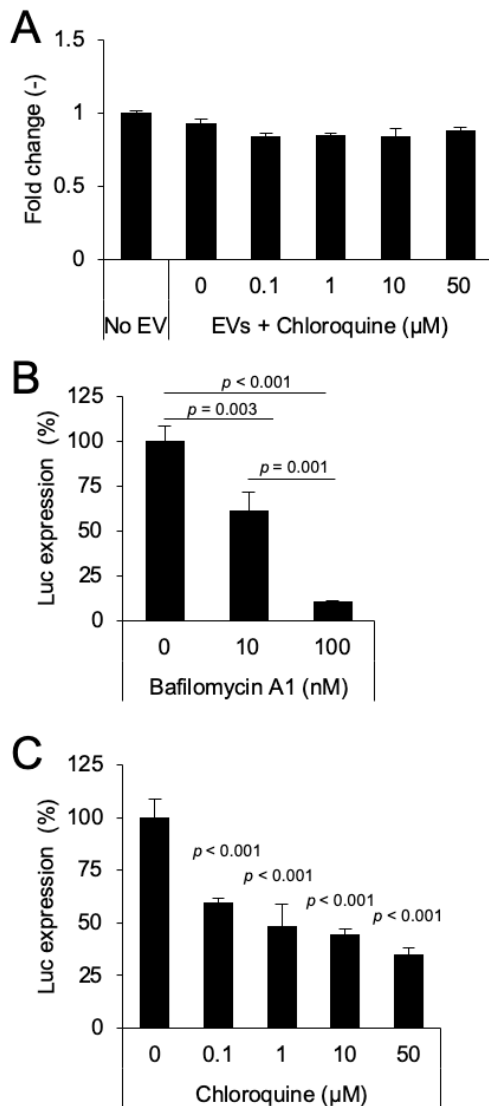


**Fig. 5** Effect of small molecule compounds on the ETTD assay.

(A) EVs (CD81-tTA) without VSV-G were applied to recipient HEK293T cells in the presence of indicated concentrations of chloroquine. NanoLuc expression level was normalized to the value of the control (no EV treatment) and is presented as fold-change.

(B) EVs (CD81-tTA) with VSV-G were applied to recipient cells in the presence of 10 or 100 nM of bafilomycin A1.

(C) EVs (CD81-tTA) with VSV-G were

301 applied to recipient cells in the presence of 0.1 to 50  $\mu$ M of chloroquine.

302 N = 3, mean  $\pm$  SD. Statistical analysis was performed using one-way ANOVA followed

303 by *post hoc* Tukey's HSD test.

304

305 In addition to potential delivery enhancers, we assessed the effect of entry

306 inhibitors using the ETTD assay. We used VSV-G-modified EVs to assess the effect of

307 compounds that are known to increase the endosomal pH and thereby inhibit the low pH-  
308 dependent fusion activity of VSV-G<sup>23,24</sup>. Bafilomycin A1 is a selective ATPase inhibitor  
309<sup>25</sup> that prevents the acidification of endosomes/lysosomes and inhibits VSV infection<sup>26</sup>.  
310 When recipient cells were treated with bafilomycin A1, membrane fusion by VSV-G-  
311 modified EVs was significantly inhibited in a dose-dependent manner (Fig. 5B). In  
312 addition, chloroquine, which is known to prevent VSV infection by increasing  
313 endosomal/lysosomal pH<sup>27</sup>, also blocked the membrane fusion of EVs (Fig. 5C). These  
314 results strongly support the application of ETTD assay in assessing pharmacological  
315 effects of a potential delivery enhancer/inhibitor of EVs.

316

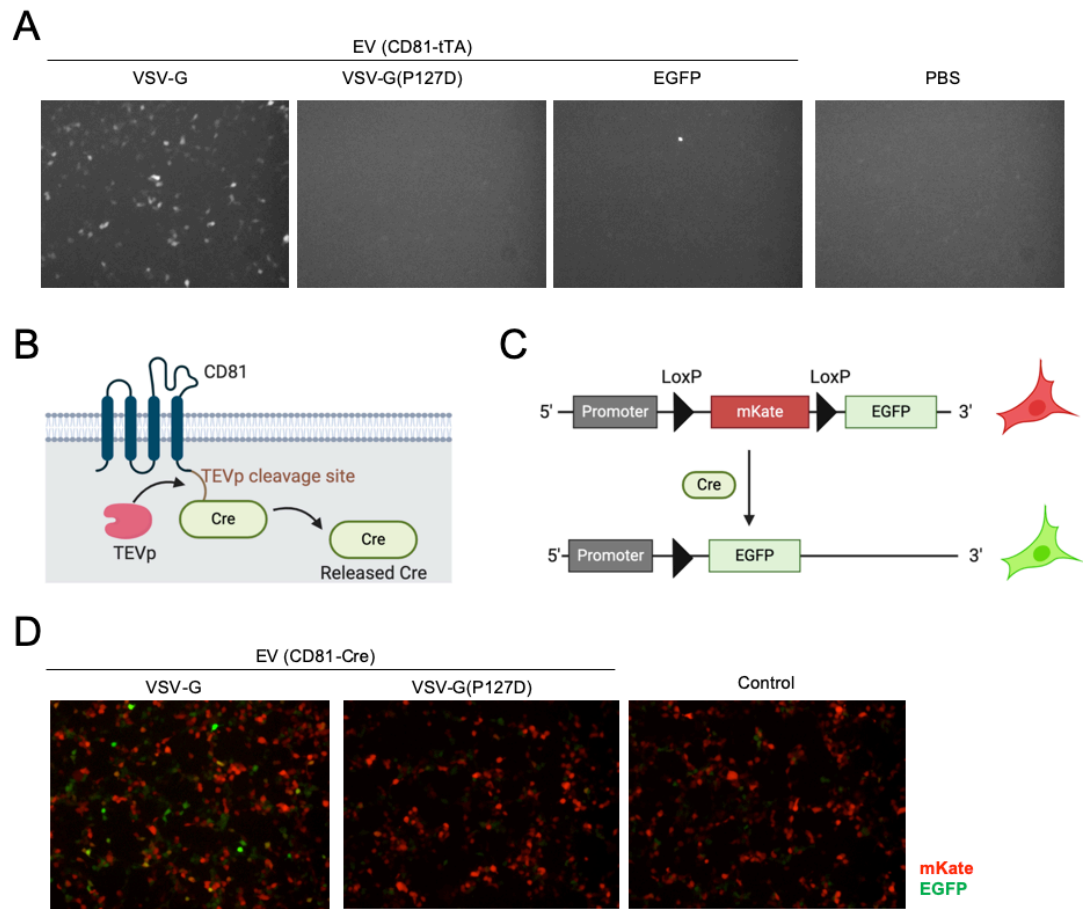
### 317 *Assessment of membrane fusion efficiency of EVs at the single-cell level*

318 For the evaluation of EV membrane fusion at the single-cell level, we changed the  
319 reporter gene from NanoLuc to EGFP. As shown in Fig. 6A, EVs containing tTA-fused  
320 CD81 and VSV-G induced EGFP expression in the recipient cells, which was consistent  
321 with previous results (Fig. 4). This assay enabled us to decipher membrane fusion  
322 efficiency at the single-cell level.

323 To further validate the general applicability of the ETTD assay, we switched the  
324 reporter gene from tTA-dependent gene expression to the expression of a floxed gene

325 dependent on Cre recombinase. The principle of the Cre-mediated reporter assay is  
326 essentially the same as that of the ETTD assay; however, the readout is driven by Cre-  
327 mediated recombination of the target gene. After the release of Cre from EV by TEVp,  
328 Cre recombinases translocate to the nucleus and induce recombination of the target  
329 plasmid (Fig. 6B & 6C). In this study, we used the mKate/EGFP reporter plasmid. The  
330 recipient cells initially expressed the red fluorescence protein mKate, but after Cre-  
331 mediated recombination, cells become EGFP positive (Fig. 6C). This assay may be more  
332 sensitive than the tTA reporter assay as even a single molecule of Cre recombinase can  
333 induce a readout in the recipient cells. As shown in Fig. 6D, EVs containing CD81-Cre  
334 with VSV-G induced EGFP positive cells, whereas EVs with VSV-G (P127D) showed  
335 almost no EGFP positive cells. This result was consistent with the results of the previous  
336 ETTD assay (Fig. 4) and again revealed that fusogenic proteins significantly increase the  
337 membrane fusion activity of EVs.

338



339

340 **Fig. 6** Fluorescence imaging-based reporter assays

341 (A) EDDT assay based on EGFP as a reporter readout. Recipient HEK293T cells were

342 transfected with plasmids encoding TRE3G-EGFP and TEVp, and treated with EVs

343 containing CD81-tTA with VSV-G (WT or P127D mutant) or EGFP (negative control).

344 After 24 h, cells were observed under a fluorescence microscope.

345 (B) Schematic representation of Cre-fused CD81.



346 (C) Schematic representation of reporter plasmid for Cre-LoxP reporter assay. After the

347 Cre cleavage, mKate gene is excised and reporter cells become EGFP positive.

348 (D) Fluorescence imaging of Cre-LoxP reporter assay. Recipient cells were treated with

349 EVs harboring CD81-Cre and VSV-G.

350

351 **Discussion**

352 In this study, we developed an ETTD assay that can evaluate the membrane fusion  
353 efficiency of EVs in recipient cells. The principle of this assay was inspired by the tango  
354 assay<sup>28</sup> that quantitatively assesses receptor activation by the recruitment of genetically  
355 engineered TEVp to the receptor, subsequent release of tTA, and expression of TRE-  
356 mediated reporter gene. In the ETTD assay, tetraspanins constrain tTA and are localized  
357 at the membrane (Fig. 2B). Once the luminal tTA is exposed to the cytoplasm following  
358 membrane fusion of the EVs and release by TEVp cleavage, recipient cells express the  
359 reporter gene (Fig. 4D). This experimental design has rendered the ETTD assay robust  
360 and sensitive by avoiding non-specific background signals.

361 The ETTD assay enables us to quantitatively assess membrane fusion efficiency  
362 and delivery mechanism of EVs. The advantages of this assay are as follows: (1) it is  
363 highly sensitive to measure the membrane fusion of EVs with a wide dynamic range  
364 owing to the very bright NanoLuc, (2) fewer confounding factors in the ETTD assay  
365 compared to conventional assays because expression of the reporter gene under the TRE  
366 promoter is highly regulated and specific to the transcription factor tTA, which does not  
367 exist in mammalian cells; and (3) it is feasible to assess the membrane fusion efficiency

368 in both the bulk cell population (NanoLuc reporter) and single-cell level (fluorescence  
369 protein reporter).

370 The very bright NanoLuc reporter gene, enables the ETTD assay to detect rare  
371 membrane fusion events in recipient cells. Because the cargo delivery efficiency of EVs  
372 is expected to be low (possibly 0.2% to 10% of recipient cells express reporter gene as a  
373 result of the cargo delivery, depending on the reporter assay <sup>15,29</sup>), the assay sensitivity  
374 must be high to capture the membrane fusion events in recipient cells. When the EVs  
375 harbor the fusogenic protein, VSV-G, EV-mediated membrane fusion was sufficient for  
376 detection in the ETTD reporter assay, whereas no detectable membrane fusion was  
377 observed in the absence of VSV-G (Fig. 4). This result reflected the low efficiency of  
378 membrane fusion in the absence of a particular membrane fusion protein. As described in  
379 previous studies, the cargo delivery efficiency of EVs is expected to be low <sup>11,15,21,30-32</sup>.  
380 However, our experiments were conducted using a combination of HEK293T donor cells  
381 and HEK293T or HeLa recipient cells. Other combinations of EV-donor cells and  
382 recipient cells should be examined to determine whether the cargo delivery efficiency is  
383 much higher in a future study.

384 We validated whether the ETTD assay precisely reflects tTA protein-mediated  
385 readout rather than mRNA transfer-dependent reporter gene expression. EVs can

386 encapsulate overexpressed mRNA in the donor cells in a passive manner and potentially  
387 transfer the mRNA to recipient cells<sup>33</sup>. Since it was postulated that unexpected EV-  
388 mediated transfer of tTA mRNA may lead to a false positive signal in the ETTD assay,  
389 recipient cells were pre-transfected with potent TetR-targeting siRNA (Fig. S2) and  
390 blocked the mRNA-mediated readout. The results clearly demonstrated that siRNA  
391 targeting TetR did not affect the assay readout, indicating the absence of mRNA-  
392 dependent tTA expression and subsequent reporter gene expression in the recipient cells  
393 (Fig. 4F).

394 Previously, membrane fusion of EVs has been evaluated by fluorescence probes  
395<sup>34</sup> or reporter proteins<sup>19,20</sup>. The former approach, especially the membrane-anchored  
396 fluorescence probes, such as R18, are known to often result in false positives due to non-  
397 specific dye transfer between lipid membranes<sup>35</sup>. Joshi et al. developed a sophisticated  
398 fluorescence imaging technique to measure membrane fusion and cargo release of EVs  
399 in recipient cells<sup>36</sup>. Their approach enabled the assessment of membrane fusion at the  
400 single-vesicle level; however, it was still difficult to distinguish the membrane fusion  
401 signal from the high background signal of the fluobodies distributed throughout the  
402 cytoplasm, and there was a limited capability in terms of throughput. The latter approach,  
403 typically using  $\beta$ -lactamase (BlaM) protein, is a time-consuming assay that requires a

404 long incubation time for the enzymatic conversion of a fluorescence substrate (7 to 16 h  
405 <sup>19,20,37</sup>). The ETTD assay, in contrast, is more feasible, sensitive, and rapid to assess the  
406 membrane fusion process of EVs in recipient cells and capable the high-throughput  
407 applications.

408         There are conflicting reports on the effect of chloroquine on EV cargo delivery  
409 in a previous study <sup>14</sup>. In this study, chloroquine was unable to enhance membrane fusion  
410 and cargo delivery of EVs (Fig. 5A), whereas a previous study showed significant  
411 improvement in the Cre delivery of EVs. The inconsistency is probably due to the  
412 differences in the experimental settings, sensitivity, and accuracy between assays. The  
413 Cre-LoxP reporter assay is a sensitive and robust method since the assay readout is driven  
414 by ideally a single Cre molecule in the recipient cell, and assay readout is exclusively  
415 dependent on the Cre-LoxP excision of target DNA. The different conclusions between  
416 these studies should be carefully interpreted and further examined in a future study. Heath  
417 et al. demonstrated that small amounts of Cre recombinase (8.9 Cre-FRB molecules per  
418 EV on average) can be passively loaded into EVs and contribute to the recombination in  
419 the recipient cells <sup>14</sup>, whereas our approach involved fusion of the Cre protein to the  
420 tetraspanin CD81 and application to the reporter recipient cells (Fig. 6B). It appears that  
421 our approach may be more convincing because the direct fusion of Cre with the EV

422 marker protein is more reliable and precisely reflects the nature of EV-mediated cargo

423 transfer.

424 **Conclusions**

425           ETTD assay is a novel functional assay to assess the mechanism of EV-mediated  
426 membrane fusion and cargo delivery in a quantitative manner. The lack of reliable  
427 functional assays in the EV field has hampered progress in its therapeutic applications<sup>38</sup>  
428 and elucidation of the underlying mechanism of cargo delivery and intercellular  
429 communication of EVs<sup>10</sup>. The ETTD assay is potentially useful for identifying unknown  
430 factors that are responsible for the cargo delivery mechanism. Using the ETTD assay,  
431 knockout or knockdown of target genes may reveal the unknown cargo delivery pathway  
432 as described in a previous study<sup>15</sup>, or possibly facilitate the discovery of a methodology  
433 that enhances membrane fusion and subsequent cargo delivery of EVs. Together with the  
434 previously reported real-time cargo delivery assay<sup>21</sup>, the ETTD assay may help advance  
435 fundamental EV research and its clinical applications.

436

437

438 **Acknowledgments**

439 We extend our gratitude to Yumi Yukawa for technical assistance in plasmid construction.

440 All illustrations in this work were created using BioRender.com.

441 This work was supported in part by JSPS KAKENHI (Grant-in-Aid for Early-

442 Career Scientists 18K18386 and 20K15790 to MS), Research Grant from JGC-

443 Scholarship (to MS), and the “Dynamic Alliance for Open Innovation Bridging Human,

444 Environment and Materials” (MEXT).

445



446 **References**

- 447 1. Nicolás-Ávila, J. A. *et al.* A Network of Macrophages Supports Mitochondrial  
448 Homeostasis in the Heart. *Cell* **183**, 94-109.e23 (2020).
- 449 2. Takahashi, A. *et al.* Exosomes maintain cellular homeostasis by excreting harmful  
450 DNA from cells. *Nat. Commun.* **8**, 15287 (2017).
- 451 3. Seo, N. *et al.* Activated CD8<sup>+</sup> T cell extracellular vesicles prevent tumour  
452 progression by targeting of lesional mesenchymal cells. *Nat. Commun.* **9**, (2018).
- 453 4. Putz, U. *et al.* The Tumor Suppressor PTEN Is Exported in Exosomes and Has  
454 Phosphatase Activity in Recipient Cells. *Sci. Signal.* **5**, ra70–ra70 (2012).
- 455 5. Bobrie, A. *et al.* Rab27a Supports Exosome-Dependent and -Independent  
456 Mechanisms That Modify the Tumor Microenvironment and Can Promote Tumor  
457 Progression. *Cancer Res.* **72**, 4920–4930 (2012).
- 458 6. Ye, S. *et al.* Tumor-derived exosomes promote tumor progression and T-cell  
459 dysfunction through the regulation of enriched exosomal microRNAs in human  
460 nasopharyngeal carcinoma. *Oncotarget* **5**, 5439–5452 (2014).
- 461 7. Mateescu, B. *et al.* Obstacles and opportunities in the functional analysis of  
462 extracellular vesicle RNA - An ISEV position paper. *J. Extracell. Vesicles* **6**,  
463 1286095 (2017).

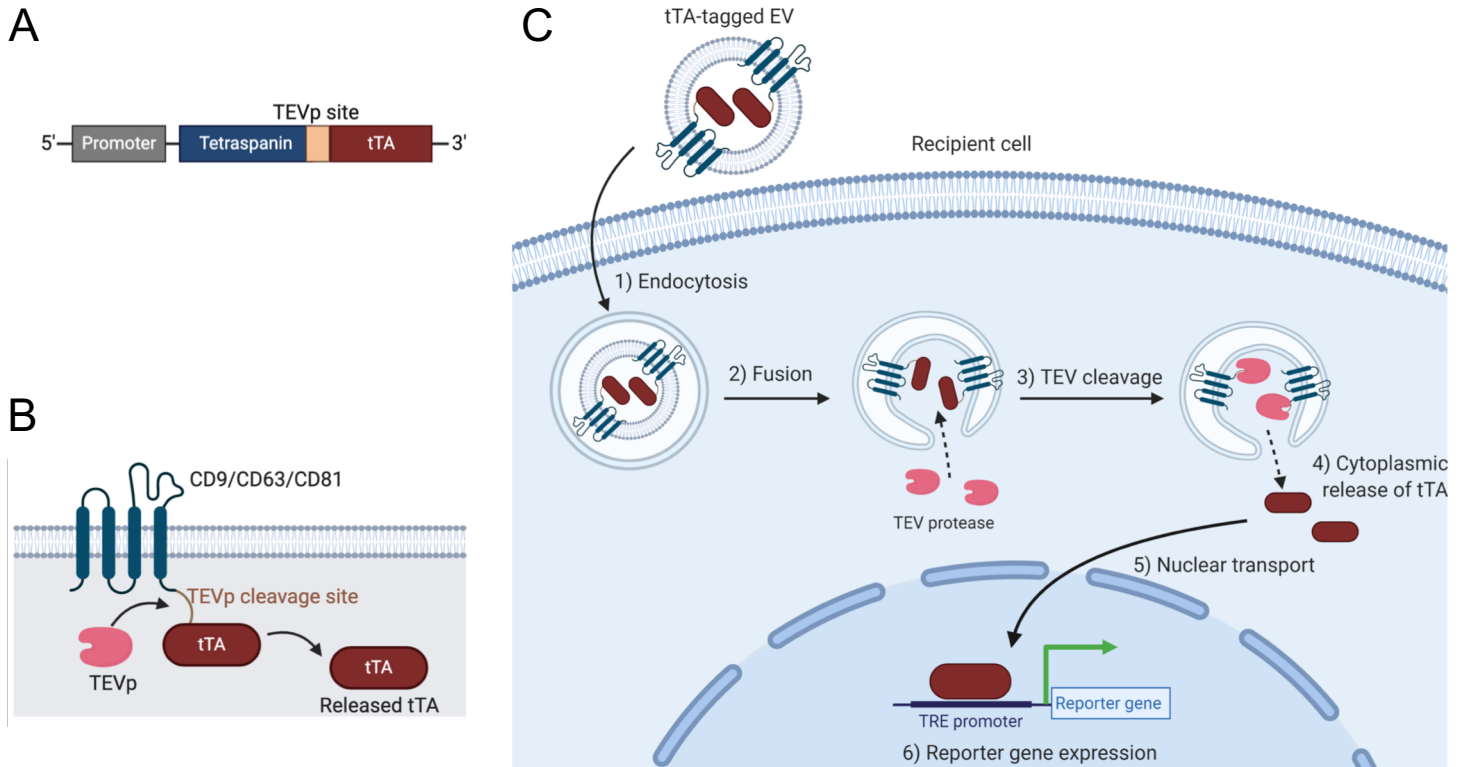
- 464 8. Whittaker, T. E., Nagelkerke, A., Nele, V., Kauscher, U. & Stevens, M. M.  
465 Experimental artefacts can lead to misattribution of bioactivity from soluble  
466 mesenchymal stem cell paracrine factors to extracellular vesicles. *J. Extracell.*  
467 *Vesicles* **9**, 1807674 (2020).
- 468 9. Somiya, M. Where does the cargo go?: Solutions to provide experimental support  
469 for the “extracellular vesicle cargo transfer hypothesis”. *J. Cell Commun. Signal.*  
470 **14**, 135–146 (2020).
- 471 10. Russell, A. E. *et al.* Biological membranes in EV biogenesis, stability, uptake, and  
472 cargo transfer: an ISEV position paper arising from the ISEV membranes and EVs  
473 workshop. *J. Extracell. Vesicles* **8**, 1684862 (2019).
- 474 11. Sutaria, D. S. *et al.* Low active loading of cargo into engineered extracellular  
475 vesicles results in inefficient miRNA mimic delivery. *J. Extracell. Vesicles* **6**,  
476 1333882 (2017).
- 477 12. Stevanato, L., Thanabalasundaram, L., Vysokov, N. & Sinden, J. D. Investigation of  
478 content, stoichiometry and transfer of miRNA from human neural stem cell line  
479 derived exosomes. *PLoS ONE* **11**, 1–13 (2016).
- 480 13. Zomer, A., Steenbeek, S. C., Maynard, C. & van Rheenen, J. Studying extracellular  
481 vesicle transfer by a Cre-loxP method. *Nat. Protoc.* **11**, 87–101 (2016).

- 482 14. Heath, N. *et al.* Endosomal escape enhancing compounds facilitate functional  
483 delivery of extracellular vesicle cargo. *Nanomed.* **14**, 2799–2814 (2019).
- 484 15. de Jong, O. G. *et al.* A CRISPR-Cas9-based reporter system for single-cell detection  
485 of extracellular vesicle-mediated functional transfer of RNA. *Nat. Commun.* **11**,  
486 (2020).
- 487 16. Kalluri, R. & LeBleu, V. S. The biology, function, and biomedical applications of  
488 exosomes. *Science* **367**, eaau6977 (2020).
- 489 17. Gibson, D. G. *et al.* Enzymatic assembly of DNA molecules up to several hundred  
490 kilobases. *Nat. Methods* **6**, 343–345 (2009).
- 491 18. Hall, M. P. *et al.* Engineered luciferase reporter from a deep sea shrimp utilizing a  
492 novel imidazopyrazinone substrate. *ACS Chem. Biol.* (2012)  
493 doi:10.1021/cb3002478.
- 494 19. Votteler, J. *et al.* Designed proteins induce the formation of nanocage-containing  
495 extracellular vesicles. *Nature* **540**, 292–295 (2016).
- 496 20. Albanese, M. *et al.* Micro RNAs are minor constituents of extracellular vesicles and  
497 are hardly delivered to target cells. *bioRxiv* 2020.05.20.106393 (2020)  
498 doi:10.1101/2020.05.20.106393.

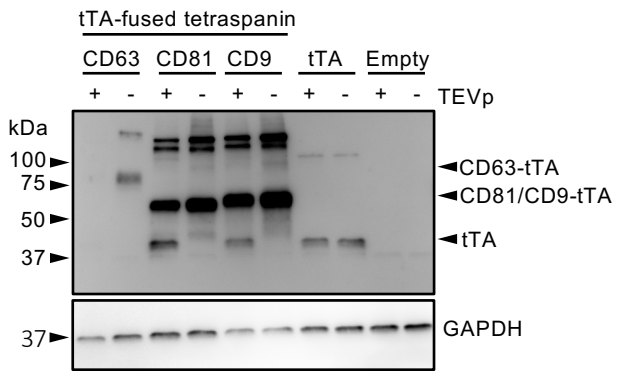
- 499 21. Somiya, M. & Kuroda, S. Real-time luminescence assay for cytoplasmic cargo  
500 delivery of extracellular vesicles. *bioRxiv* 2020.10.16.341974 (2020)  
501 doi:10.1101/2020.10.16.341974.
- 502 22. Fredericksen, B. L. & Whitt, M. A. Vesicular Stomatitis Virus Glycoprotein  
503 Mutations That Affect Membrane Fusion Activity and Abolish Virus Infectivity. *J*  
504 *VIROL* 9.
- 505 23. Ci, Y., Yang, Y., Xu, C. & Shi, L. Vesicular stomatitis virus G protein  
506 transmembrane region is crucial for the hemi-fusion to full fusion transition. *Sci.*  
507 *Rep.* **8**, 10669 (2018).
- 508 24. Kim, I. S. *et al.* Mechanism of membrane fusion induced by vesicular stomatitis  
509 virus G protein. *Proc. Natl. Acad. Sci.* **114**, E28–E36 (2017).
- 510 25. Bowman, E. J., Siebers, a & Altendorf, K. Bafilomycins: a class of inhibitors of  
511 membrane ATPases from microorganisms, animal cells, and plant cells. *Proc. Natl.*  
512 *Acad. Sci. U. S. A.* **85**, 7972–6 (1988).
- 513 26. Yonezawa, A., Cavrois, M. & Greene, W. C. Studies of Ebola Virus Glycoprotein-  
514 Mediated Entry and Fusion by Using Pseudotyped Human Immunodeficiency Virus  
515 Type 1 Virions: Involvement of Cytoskeletal Proteins and Enhancement by Tumor  
516 Necrosis Factor Alpha. *J. Virol.* **79**, 918–926 (2005).

- 517 27. Sakata, M. *et al.* Analysis of VSV pseudotype virus infection mediated by rubella  
518 virus envelope proteins. *Sci. Rep.* **7**, 11607 (2017).
- 519 28. Barnea, G. *et al.* The genetic design of signaling cascades to record receptor  
520 activation. *Proc. Natl. Acad. Sci.* **105**, 64–69 (2008).
- 521 29. Zomer, A. *et al.* In vivo imaging reveals extracellular vesicle-mediated  
522 phenocopying of metastatic behavior. *Cell* **161**, 1046–1057 (2015).
- 523 30. Hung, M. E. & Leonard, J. N. A platform for actively loading cargo RNA to  
524 elucidate limiting steps in EV-mediated delivery. *J. Extracell. Vesicles* **1**, 1–13  
525 (2016).
- 526 31. Stremersch, S. *et al.* Comparing exosome-like vesicles with liposomes for the  
527 functional cellular delivery of small RNAs. *J. Controlled Release* **232**, 51–61  
528 (2016).
- 529 32. Wang, Q. *et al.* ARMMs as a versatile platform for intracellular delivery of  
530 macromolecules. *Nat. Commun.* **9**, (2018).
- 531 33. Lai, C. P. *et al.* Visualization and tracking of tumour extracellular vesicle delivery  
532 and RNA translation using multiplexed reporters. *Nat. Commun.* **6**, 7029 (2015).
- 533 34. Parolini, I. *et al.* Microenvironmental pH Is a Key Factor for Exosome Traffic in  
534 Tumor Cells. *J. Biol. Chem.* **284**, 34211–34222 (2009).

- 535 35. Wunderli-Allenspach, H. & Ott, S. Kinetics of fusion and lipid transfer between  
536 virus receptor-containing liposomes and influenza viruses as measured with the  
537 octadecylrhodamine B chloride assay. *Biochemistry* **29**, 1990–1997 (1990).
- 538 36. Joshi, B. S., de Beer, M. A., Giepmans, B. N. G. & Zuhorn, I. S. Endocytosis of  
539 Extracellular Vesicles and Release of Their Cargo from Endosomes. *ACS Nano*  
540 *acsnano.9b10033* (2020) doi:10.1021/acsnano.9b10033.
- 541 37. Cavrois, M., de Noronha, C. & Greene, W. C. A sensitive and specific enzyme-  
542 based assay detecting HIV-1 virion fusion in primary T lymphocytes. *Nat.*  
543 *Biotechnol.* **20**, 1151–1154 (2002).
- 544 38. Nguyen, V. V. T., Witwer, K. W., Verhaar, M. C., Strunk, D. & Balkom, B. W. M.  
545 Functional assays to assess the therapeutic potential of extracellular vesicles. *J.*  
546 *Extracell. Vesicles* **10**, (2020).



**A**



**B**

